

# **Modulation in the motion of an autonomous molecular-machine assembly caused by the hysteresis memorising the directionality of the applied light**

Yoshiyuki Kageyama,\* Makiko Matsuura, and Daisuke Yazaki

## **Introductory Paragraph**

Living organisms show self-sustained motion and make behavioural decisions in response to their environment. Recently, creation of animal-like macroscopic dynamics using molecular machines takes large attentions.<sup>1,2</sup> However, it is unclear how such systems can acquire the ability to make behavioural decisions in response to their environment. We have previously reported a light-driven self-oscillation of a crystal<sup>3</sup> and its behavioural complication under the polarised driving light.<sup>4</sup> Here, we reveal that the complexity in apparent behaviour of the material not only reflects the orientation of the crystal relative to the incident light but also reflects adaptation, i.e., the components remember the polarity of the preceding light input. Our results provide a new concept, i.e., collaboration between a motor molecule to achieve self-sustaining motion and a responsive machine for storing information to realise self-governed dynamics in a multimolecular architecture.

## **Main**

The bottom-up construction of molecular machines to create a life-like autonomous architecture represents a longstanding challenge in molecular science and nanotechnology.<sup>2,5,6</sup> The fundamental requirement for such intelligent matter is self-repetitive mechanical work at the macroscopic level. An inanimate chemical system will generally achieve a balanced state of chemical reactions, known as an equilibrium or a stationary state, in which the system maintains a static composition determined by kinetic coefficients.<sup>7,8</sup> Therefore, to make and control mechanical functions of multimolecular materials repetitively, humans give changes in conditions surrounding the materials to change the kinetic coefficients. To autonomously avoid achieving such a balanced state, the kinetic coefficients in the system must oscillate or fluctuate automatically.<sup>8,9</sup> It is commonly known as a feedback mechanism. Indeed, the bottom-up construction of chemical objects with continuous autonomous dynamic behaviour has recently been realised via autocatalytic processes with time-delayed feedback at the flask level<sup>10,11</sup> and the molecular assembly level.<sup>12,13</sup> However, it remains uncertain how such active

molecular systems could acquire self-governed features with intelligence akin to that of living organisms.

Previously, we have reported the light-driven self-sustained oscillation of a co-crystal composed of the azobenzene derivative 6-[4-(phenylazo)phenoxy]hexanoic acid (**1**) and oleic acid in a  $\sim 3:2$  molar ratio.<sup>3,4,14</sup> In our first paper, we revealed that the self-sustaining oscillation is realised by the fact that the photoisomerisation-triggered phase transition causes switching of the kinetic coefficients of the photoisomerisation.<sup>3</sup> An advantage of this mechanism is that external information, such as the position or polarisation of the energy source, is not critical,<sup>15</sup> unlike in the mechanisms of other continuously moving photomechanical materials working under directional lights.<sup>16-28</sup> Therefore, regardless of whether it adopts a “standing” or “lying” orientation with respect to the incident light, the crystal continues to flip.<sup>3</sup> Furthermore, the crystals’ self-propulsion in water is not determined by the direction of the incident light, but instead by their anisotropic shape.<sup>14</sup> Conversely, when a directional energy source is used, the original self-sustaining oscillation of the object is disturbed, because the reaction probability is affected by the directionality. Indeed, we have previously reported that the properties of the repetitive motion vary in response to changes in the polarisation angle.<sup>4</sup> In that paper, we also revealed the single-crystal structure of a polymorph of **1**, whose powder X-ray diffraction pattern was similar to that of the co-crystal. According to the crystal structure with six crystallographically independent azobenzene molecules, we concluded that the co-crystal consisted of four crystallographically independent azobenzene molecules and two crystallographically independent molecules of oleic acid (Fig. 1), whereby one of the azobenzene molecule acts as the oscillation generator while the other azobenzene molecules regulate the flipping properties. In the present paper, the frequency of self-oscillation of the same co-crystals under polarised light is examined, and the origin of the polarised-light-triggered variation in the frequency is revealed with the support of a mathematical analysis of the reaction kinetics. Moreover, we discovered that a novel type of hysteresis due to the regulatory azobenzene molecules “remembering” information from the previous external operation also contributes to the diversity of the flipping properties.

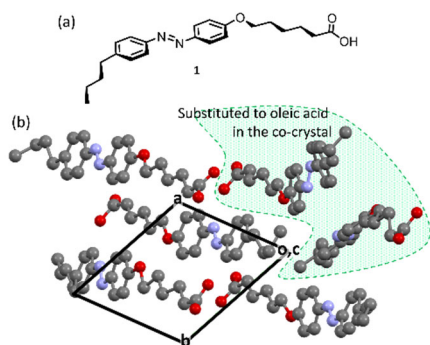


**Fig. 1** Schematic illustration of the (a) chemical formula of **1** and (b) unit cell of single crystals of **1**, which crystallise in the space group  $P_1$  (for the crystallographic data, see: ref. 4)<sup>§</sup>; hydrogen atoms in **1** have been omitted for clarity. The structure of the co-crystals between **1** and oleic acid was tentatively assigned to be same as that illustrated above, except for the two encircled molecules of **1**, which lack effective dipole-dipole interactions around the ether oxygen and are thus presumed to be replaced by oleic acid.<sup>4</sup>

A crystal composed of the *trans*-isomer of **1** and oleic acid (for details on the synthesis of the co-crystal, see the *Method* section in SI and ref. 4) was placed on a glass slide as an aqueous dispersion. The frequency of the resulting self-oscillation is shown as a polar plot against the polarisation angle of the blue excitation light ( $\lambda_{\text{ex}} = 435 \text{ nm}$ ) (Fig. 2a). The excitation light was applied vertically (i.e., perpendicular to the face of the glass slide), and its polarisation azimuth was defined with respect to the micrographic view, with correction if the crystal rotated. The crystals oscillated in vertical direction; the oscillation was detected as the repeated observation of an in-focus flat object and an out-of-focus bent object (Fig. 2b). In the experiment, we first exposed the crystal to unpolarised light ( $\lambda_{\text{ex}} = 435 \text{ nm}$ ) for 5 s to generate the self-oscillation, and then measured the oscillation frequency under exposure to polarised light ( $\lambda_{\text{ex}} = 435 \text{ nm}$ ). Generally, the excitation probability of a molecule as a function of the light polarity is proportional to  $|\mathbf{M}|^2 \cos^2 \Delta\theta$ , where  $\mathbf{M}$  is the transition moment of the molecule and  $\Delta\theta$  is the differential angle between the azimuth angle of  $\mathbf{M}$  and that of the light polarisation.<sup>29</sup> However, the shape of the experimentally obtained polar plot of the frequency was not proportional to  $\cos^2 \Delta\theta$ , i.e., the forbidden angular span was wide and the line-symmetry was broken. Furthermore, even in cases in which the frequency of the flipping was similar for different light-polarisation angles, the time profile of the flipping was different. Fig. 2c presents the time profile of the flipping motion of the same crystal under  $100^\circ$  and  $170^\circ$  polarised light. The duration ratio of the bent shape to the flat shape ( $Dr$ ) was 1.4 at  $170^\circ$  and 0.96 at  $100^\circ$ .

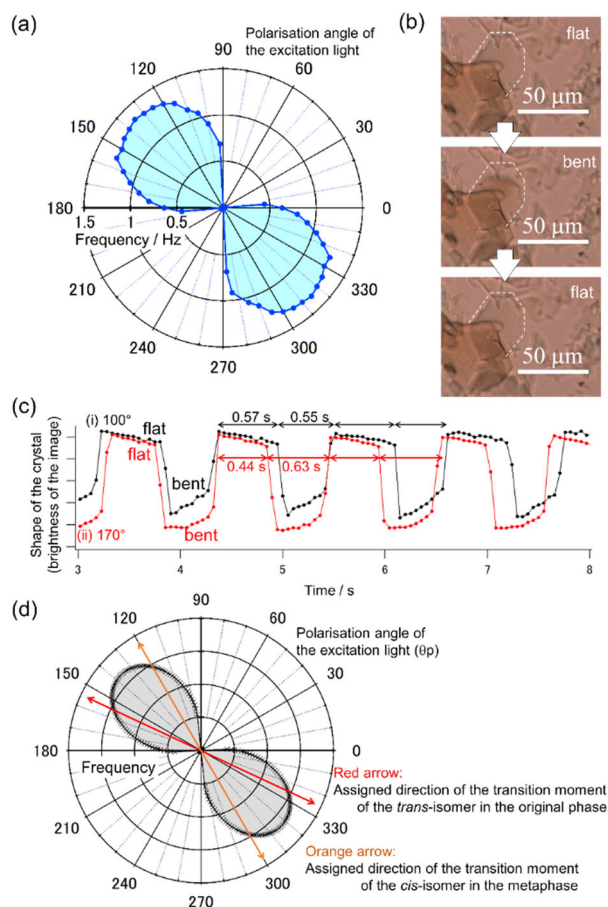


**Fig. 2** (a) Frequency of the self-oscillation of a crystal under polarised blue light ( $\lambda_{\text{ex}} = 435$  nm), obtained after irradiation with unpolarised blue light ( $\lambda_{\text{ex}} = 435$  nm) for 5 s. The frequency resolution is approximately 0.05 Hz due to the frame speed of the video used to generate this image (for details, see Movie S1 in the Supplementary Information (SI)). (b) Sequential microscopic images (interval: 0.42 s) of the oscillatory flipping of the crystal under excitation light with a polarisation angle of  $140^\circ$ . The dashed lines are guides for the eye. (c) Time profiles of the self-oscillation under light with a polarisation angle of  $100^\circ$  and  $170^\circ$ , respectively. The vertical axis is the brightness of a part of the crystal in the video used to generate this image (for details, see Movie S1 in the SI) and indicates the state of the crystal. (d) Simulated results using  $\theta_{\text{to}} = 155^\circ$ ,  $\theta_{\text{co}} = 15^\circ$ ,  $\theta_{\text{m}} = 75^\circ$ , and  $\theta_{\text{cm}} = 120^\circ$  in the equations shown in the appendix. Data were calculated for polarisation angles ( $\theta_{\text{p}}$ ) intervals of 1 degree.  $A_{\text{o}}$ ,  $B_{\text{o}}$ ,  $A_{\text{m}}$ , and  $B_{\text{m}}$  were set to 0.005, 0.004, 0.001, and 0.02, respectively. The  $R$  values at the thresholds for the “original-phase-to-metaphase transition” and the “metaphase-to-original-phase transition” were assigned as 0.5 and 0.05, respectively. These values were not optimised.

These results originate from the fact that the oscillation is realised by both the *trans*-isomer-decreasing photoisomerisation of the generator azobenzene molecule at the original crystalline phase (flat shape) and the *cis*-isomer-decreasing photoisomerisation of the generator azobenzene molecule at the metaphase crystal (bent shape).<sup>3,4</sup> Indeed, using the kinetic equations based on the proposed mechanism described in the appendix in the Supplementary Information (SI), we were able to successfully simulate the experimental results (Fig. 2d); in the simulation, the azimuth angles of the transition moments of the *trans*-isomer in the original phase and the *cis*-isomer in the metaphase were assigned as 155° and 120°, respectively. In the model, *trans*-to-*cis* and *cis*-to-*trans* photoisomerisation sufficient to generate the self-oscillation occurs between 95° and 185°; the excitation of the *cis*-isomer in the metaphase occurs efficiently at the smaller angle, resulting in a smaller  $Dr$ . In contrast, the excitation of the *trans*-isomer in the original phase or of the *cis*-isomer in the metaphase, or both of them were insufficient for realising self-oscillation at around 60° and 30°, respectively.

The difference between the angle of the polarisation light and the azimuth angles of the transition moments of the *trans*-isomer in the original phase and the *cis*-isomer in the metaphase determines whether self-oscillation occurs or not. Therefore, if the crystal tilts, the angle between the azimuthal angles changes and the apparent dependence on the polarisation angle of the light is altered. Fig. 3 presents the results for another crystal, the plane of which was oriented in an oblique vertical direction. Even though the shape of the polar plot was very different from that in Fig. 2, the experimental result was well simulated by employing the same model with different azimuth angles. Thus, one reason that the behaviour of the crystals under polarised excitation light differs from crystal to crystal is the different relative orientations of the crystals with respect to the incident light.

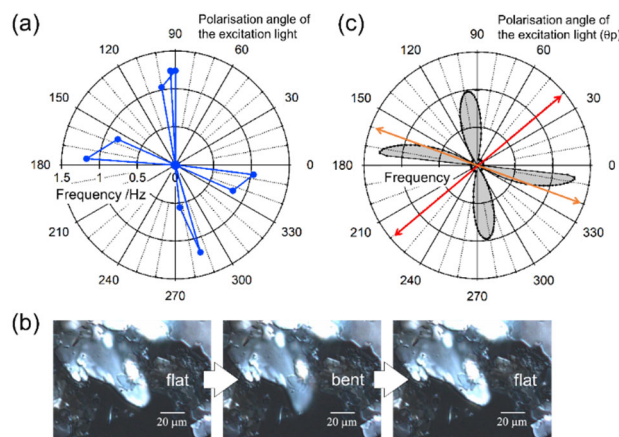


**Fig. 3** (a) Frequency of the self-oscillation of a tilted crystal under polarised blue light ( $\lambda_{\text{ex}} = 435 \text{ nm}$ ), obtained after irradiation with unpolarised blue light ( $\lambda_{\text{ex}} = 435 \text{ nm}$ ) for 5 s. The

frequency resolution is approximately 0.05 Hz due to the frame speed of the video used to generate this image (for details, see Movie S4 in the SI). (b) Sequential microscopic images (intervals: 0.36 s) of the oscillatory flipping of the crystal under excitation light with a polarisation angle of  $90^\circ$ . (c) Simulated results using  $\theta_{to} = 40^\circ$ ,  $\theta_{co} = 37^\circ$ ,  $\theta_{tm} = 0^\circ$ , and  $\theta_{cm} = 160^\circ$  in the equations shown in the appendix in the SI. Red and orange arrows indicate the direction of  $\theta_{to}$  and  $\theta_{cm}$ , respectively. For the other parameters in the simulation, the values given in Fig. 2 were employed. These values were not optimised.

### Hysteresis due to the history of the polarised-light rotation

Next, we measured the flipping frequency of the crystal used for the measurements in Fig. 2 while rotating the polarisation angle by  $5^\circ$  every 5 s, without exposing the crystal to unpolarised light during the experiment. As shown in Fig. 4a, the oscillation frequency differed depending on whether the polarisation angle was rotated clockwise or counterclockwise.

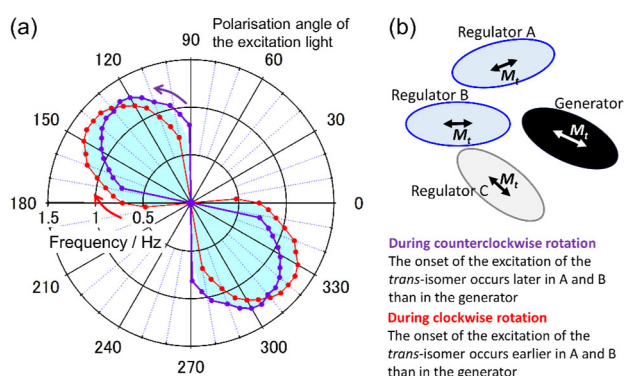


**Fig. 4** (a) Frequency of the self-oscillation of the crystal shown in Fig. 2 when the polarisation angle of the blue light was changed stepwise in increments or decrements of  $5^\circ$  (for details, see Movies S2 and S3 in the SI). The cyan-coloured area indicates the results shown in Fig. 2. (b) Schematic illustration for the explanation of the hysteresis observed with the polarisation rotation of the excited light. In the crystal, azobenzene molecules (represented as ellipses) of different symmetry are present, each with a transition moment in a different direction (represented as arrows in the ellipses). The rotation direction of the polarisation angle determines the order in which the azobenzene molecules are photoexcited, and therefore the state of the crystal varies with the rotational direction.

Based on the crystal structure reported in our previous paper (Fig. 1),<sup>4</sup> we can hypothesise that the isomer ratio of the regulator molecules, which varies with the polarised

light supplied, changes the frequency of the self-oscillation driven by the generator molecule. The direction of each transition moment of the regulator azobenzene molecules and the generator azobenzene molecule is different. Therefore, the rotational direction of the polarisation angle determines whether the regulator molecules begin to accept the polarisation light efficiently before or after the generator molecules do (Fig. 4b). This is caused by a difference in the isomer ratio of the regulator molecules that depends on the history of the rotational direction and consequently changes the character of the crystal. Thus, the frequency should change with the rotational direction of the polarisation.

As seen in the experimental results and as expected based on the above discussion, the frequency of self-oscillation reflects the history of an external operation, i.e., the rotation of the polarisation angle of the excitation light. In other words, the hysteresis of the self-oscillation is due to the crystal storing the received information. The hysteresis varies from crystal to crystal, as shown in Figs. S3–S5 in the SI, but the origin of the hysteresis seems to be the same, i.e., the observed differences are simply due to the different orientations and shapes of the crystals. Quantification of the isomerisation ratio of the regulator azobenzene molecules would be the best way to confirm this hypothesis, albeit that we have so far been unable to measure the components in such small crystals despite our best efforts and the lack of appropriate analytical techniques.

The polarisation dependence of the blue-light-driven self-oscillation of a crystal that shows stable self-oscillation under unpolarised blue light was analysed in this paper. The frequency of the light-driven self-oscillation varied with the polarisation angle of the driving light and its rotational direction. As the oscillation is the result of multiple photoexcitation processes, the range of the polarisation angles over which the self-oscillation occurs is narrower than that of a typical photochemical process. In addition, the azimuth angles of the transition moments are different for each crystal because the orientation of the crystals relative to the incident light varies, and accordingly, the polarisation-angle responsivity of the self-oscillation varies. It is noteworthy that the crystals exhibit stable self-oscillation under unpolarised blue light. This stable self-oscillation is disturbed by the directional energy supply, which results in complicated behaviour in response to polarised light, as shown in this report. This stands in contrast to other stimulus-responsive materials, in which morphological change has been achieved by de-symmetrising their shape-change via applying a directional energy source.

Furthermore, as the light-polarity information is stored as the isomer compositions of the regulator molecules, the frequency of the self-oscillation differs depending on the order of external operations. These results show that adaptation to or storage of the external operations can induce hysteresis in the autonomous dynamics of a molecular assembly.

Therein, the non-generator machine plays a key role. This concept can achieve short-term memory in life-like autonomous systems constructed from very small molecular machines, in which molecular motors for continuous dynamic behaviour and molecular machines to sense the environment work synergistically.

### Author Contributions

Y.K. designed and performed the experimental study and mathematical analysis and prepared the manuscript. M.M. and D.Y. supported the experiments and movie analysis.

### Conflicts of interest

There are no conflicts to declare.

### Acknowledgements

This work was supported by JSPS KAKENHI grant JP18H05423 within the Scientific Research on Innovative Areas "Molecular Engine". Y.K. thanks Dr. Yasuaki Kobayashi for his fruitful discussions.

### Notes and references

§ Crystallographic data of **1**, which is an analogue of the co-crystal shown in this paper, is available from CCDC (Reg. No. 183362).

- 1 Lancia, F., Ryabchun, A. & Katsonis, N. Life-like motion driven by artificial molecular machines. *Nat. Rev. Chem.* **3**, 536-551 (2019). <https://doi.org/10.1038/s41570-019-0122-2>
- 2 Lehn, J.-M. Perspectives in Chemistry—Steps towards Complex Matter. *Angew. Chem. Int. Ed.* **52**, 2836-2850 (2013). <https://doi.org/10.1002/anie.201208397>
- 3 Ikegami, T., Kageyama, Y., Obara, K. & Takeda, S. Dissipative and Autonomous Square-Wave Self-Oscillation of a Macroscopic Hybrid Self-Assembly under Continuous Light Irradiation. *Angew. Chem. Int. Ed.* **55**, 8239-8243 (2016). <https://doi.org/10.1002/anie.201600218>
- 4 Kageyama, Y. *et al.* Light-Driven Flipping of Azobenzene Assemblies-Sparse Crystal Structures and Responsive Behaviour to Polarised Light. *Chem-Eur J* **26**, 10759-10768 (2020). <https://doi.org/10.1002/chem.202000701>



- 5 Feynman, R. Infinitesimal machinery. *J. Microelectromech. Syst.* **2**, 4-14 (1993). <https://doi.org/10.1109/84.232589>
- 6 Iino, R., Kinbara, K. & Bryant, Z. Introduction: Molecular Motors. *Chem. Rev.* **120**, 1-4 (2020). <https://doi.org/10.1021/acs.chemrev.9b00819>
- 7 Goldup, S. & Aprahamian, I. Off Detailed Balance: Non-Equilibrium Steady States in Catalysis, Molecular Motors and Supramolecular Materials *ChemRxiv* (2022). <https://doi.org/10.26434/chemrxiv-2022-49s4d>
- 8 Kageyama, Y. Robust Dynamics of Synthetic Molecular Systems as a Consequence of Broken Symmetry. *Symmetry* **12**, 1688 (2020).
- 9 Kageyama, Y. & Maruta, G. Potential curves illustrating a dissipative self-assembly system and the meaning of away-from-equilibrium. *arXiv*, 2211.06147 (2022). <https://doi.org/10.48550/arXiv.2211.06147>
- 10 Howlett, M. G., Engwerda, A. H. J., Scanes, R. J. H. & Fletcher, S. P. An autonomously oscillating supramolecular self-replicator. *Nat. Chem.* **14**, 805-810 (2022). <https://doi.org/10.1038/s41557-022-00949-6>
- 11 Leira-Iglesias, J., Tassoni, A., Adachi, T., Stich, M. & Hermans, T. M. Oscillations, travelling fronts and patterns in a supramolecular system. *Nat. Nanotechnol.* **13**, 1021-1027 (2018). <https://doi.org/10.1038/s41565-018-0270-4>
- 12 Hardy, M. D. *et al.* Self-reproducing catalyst drives repeated phospholipid synthesis and membrane growth. *Proc. Nat'l. Acad. Sci. USA* **112**, 8187-8192 (2015). <https://doi.org/10.1073/pnas.1506704112>
- 13 Takahashi, H. *et al.* Autocatalytic membrane-amplification on a pre-existing vesicular surface. *Chem. Commun.* **46**, 8791-8793 (2010). <https://doi.org/10.1039/C0CC02758H>
- 14 Obara, K., Kageyama, Y. & Takeda, S. Self-Propulsion of a Light-Powered Microscopic Crystalline Flapper in Water. *Small* **18**, 2105302 (2022). [https://doi.org:https://doi.org/10.1002/sml.202105302](https://doi.org/https://doi.org/10.1002/sml.202105302)
- 15 Kageyama, Y. Light-Powered Self-Sustainable Macroscopic Motion for the Active Locomotion of Materials. *ChemPhotoChem* **3**, 327-336 (2019). <https://doi.org/10.1002/cptc.201900013>
- 16 Zhang, H. *et al.* Feedback-controlled hydrogels with homeostatic oscillations and dissipative signal transduction. *Nat. Nanotechnol.* **17**, 1303-1310 (2022). <https://doi.org/10.1038/s41565-022-01241-x>
- 17 Gelebart, A. H. *et al.* Making waves in a photoactive polymer film. *Nature* **546**, 632-636 (2017). <https://doi.org/10.1038/nature22987>
- 18 Uchida, E., Azumi, R. & Norikane, Y. Light-induced crawling of crystals on a glass

- surface. *Nat. Commun.* **6**, 7310 (2015). <https://doi.org/10.1038/ncomms8310>
- 19 Yamada, M. *et al.* Photomobile polymer materials: Towards light-driven plastic motors. *Angew. Chem. Int. Ed.* **47**, 4986-4988 (2008). <https://doi.org/10.1002/anie.200800760>
- 20 White, T. J. *et al.* A high frequency photodriven polymer oscillator. *Soft Matter* **4**, 1796 (2008). <https://doi.org/10.1039/b805434g>
- 21 Suzuki, M. & Nakano, H. Moving Fragments of Photochromic Molecular Glass of 4-[Bis(9,9-dimethylfluoren-2-yl)amino]-4'-cyanoazobenzene. *J. Photopolym. Sci. Technol.* **25**, 159-160 (2012). <https://doi.org/10.2494/photopolymer.25.159>
- 22 Hu, Z., Li, Y. & Lv, J.-a. Phototunable self-oscillating system driven by a self-winding fiber actuator. *Nat. Commun.* **12**, 3211 (2021). <https://doi.org/10.1038/s41467-021-23562-6>
- 23 Zeng, H. *et al.* Light-fuelled freestyle self-oscillators. *Nat. Commun.* **10**, 5057 (2019). <https://doi.org/10.1038/s41467-019-13077-6>
- 24 Zhao, Y. *et al.* Soft phototactic swimmer based on self-sustained hydrogel oscillator. *Sci. Robot.* **4**, eaax7112 (2019). <https://doi.org/doi:10.1126/scirobotics.aax7112>
- 25 Yang, L. *et al.* An Autonomous Soft Actuator with Light-Driven Self-Sustained Wavelike Oscillation for Phototactic Self-Locomotion and Power Generation. *Adv. Funct. Mat.* **30**, 1908842 (2020). [https://doi.org:https://doi.org/10.1002/adfm.201908842](https://doi.org/https://doi.org/10.1002/adfm.201908842)
- 26 Wang, J. *et al.* Light-driven autonomous self-oscillation of a liquid-crystalline polymer bimorph actuator. *J. Mat. Chem. C* **9**, 12573-12580 (2021). <https://doi.org/10.1039/D1TC02891J>
- 27 Pilz da Cunha, M. *et al.* A self-sustained soft actuator able to rock and roll. *Chem. Commun.* **55**, 11029-11032 (2019). <https://doi.org/10.1039/C9CC05329H>
- 28 Zibaei, R., Zakerhamidi, M. S., Korram, S. & Ranjkesh, A. Effects of polarized light on the optical and self-oscillation behaviors of liquid crystal network polymers. *J. Mat. Chem. C* **9**, 14908-14915 (2021). <https://doi.org/10.1039/D1TC03870B>
- 29 Montalti, M., Credi, A., Prodi, L. & Gandolfi, M. T. *Handbook of Photochemistry* 3edn, (CRC Press, 2006).

Supplementary Information  
for  
Modulation in the motion of an autonomous molecular-machine assembly caused by the  
hysteresis in response to the directionality of the applied light

Yoshiyuki Kageyama, Makiko Matsuura, and Daisuke Yazaki  
Faculty of Science, Hokkaido University

Table of contents:

**Appendix**     Kinetic equations for simulation (p. S3)

**Experimental Methods** (p. S5)

**Fig. S1.** Simulated time profile of the isomer ratio of the generator molecule for the crystal shown in Fig. 2. (p. S6)

**Fig. S2.** An example of the results of another crystal. (p. S7)

**Fig. S3.** Simulation and hysteresis behaviour for the crystal shown in Fig. S2. (p. S8)

**Fig. S4.** Hysteresis behaviour of the crystal shown in Fig. 3. (p. S9)

**Fig. S5.** Hysteresis behaviour of another crystal. (p. S10)

**Movie S1.** Self-oscillation of the crystal shown in Fig. 2 under polarised blue light. Before irradiation with polarised light, the crystal was irradiated with unpolarised blue light.

**Movie S2.** Self-oscillation of the crystal shown in Fig. 4 under polarised blue light. The polarisation angle was rotated counterclockwise.

**Movie S3.** Self-oscillation of the crystal shown in Fig. 4 under polarised blue light. The polarised angle was rotated clockwise.

**Movie S4.** Self-oscillation of the crystal shown in Fig. 3 under polarised blue light. Before irradiation with polarised light, the crystal was irradiated with unpolarised blue light.

**Movie S5.** Self-oscillation of the crystal shown in Fig. S4 under polarised blue light. The polarisation angle was rotated counterclockwise.

**Movie S6.** Self-oscillation of the crystal shown in Fig. S4 under polarised blue light. The polarised angle was rotated clockwise.

**Movie S7.** Self-oscillation of the crystal shown in Fig. S2 under polarised blue light. Before irradiation with polarised light, the crystal was irradiated with unpolarised blue light.

**Movie S8.** Self-oscillation of the crystal shown in Fig. S3 under polarised blue light. The polarisation angle was rotated counterclockwise.

**Movie S9.** Self-oscillation of the crystal shown in Fig. S3 under polarised blue light. The polarised angle was rotated clockwise.

**Movie S10.** Self-oscillation of the crystal shown in Fig. S5 under polarised blue light. The polarisation angle was rotated back-and-forth from  $45^\circ$  to  $65^\circ$ .

**Movie S11.** Self-oscillation of the crystal shown in Fig. S5 under polarised blue light. The polarised angle was rotated back-and-forth from  $75^\circ$  to  $55^\circ$ .

## Appendix

For the reversible photoisomerisation between the *trans*- and *cis*-isomers of azobenzene (reaction equation (1)), we can establish coarse-grained reaction rate equations (2) and (3), wherein thermal processes are ignored.



$$\frac{d}{dt}R = \alpha - (\alpha + \beta)R \quad (2)$$

$$\Delta R = \int_{t_0}^{t_1} \frac{d}{dt}R dt = \int_{t_0}^{t_1} (\alpha - (\alpha + \beta)R) dt \quad (3)$$

In these expressions,  $\alpha$  and  $\beta$  are the kinetic coefficients of the *trans*-to-*cis* and *cis*-to-*trans* photoisomerisation, respectively,  $R$  is the fraction of the *cis*-isomer, and  $\Delta R$  is the difference in  $R$  between time  $t_0$  and time  $t_1$ . Each kinetic coefficient is multiplied by the quantum yield of isomerisation ( $\Phi$ ), the excitation probability, and the light intensity ( $I$ ). As mentioned in the main text, generally, the excitation probability is proportional to  $|\mathbf{M}|^2 \cos^2 \Delta\theta$ . Therefore,  $\alpha$  and  $\beta$  can be expressed as shown in equations (4) and (5).

$$\alpha = C \times \Phi_t |\mathbf{M}_t|^2 \cos^2(\theta_t - \theta_p) I = A \cos^2(\theta_t - \theta_p) \quad (4)$$

$$\beta = D \times \Phi_c |\mathbf{M}_c|^2 \cos^2(\theta_c - \theta_p) I = B \cos^2(\theta_c - \theta_p) \quad (5)$$

where  $\theta_p$  is the polarisation angle of the light, which is irradiated from the vertical direction,  $\theta$  is the azimuth angle of the transition moment, and  $A$ – $D$  are constants that depend on the elevation angle of  $\mathbf{M}$ . The subscripts  $t$  and  $c$  indicate the *trans*-isomer and *cis*-isomer, respectively.

In the self-oscillating crystal, the kinetic parameters differ between the original phase and the metaphase. Herein, we consider the behaviour of the generator molecule. The phase transitions are

triggered when  $R$ , the *cis*-isomer fraction, reaches the respective threshold ( $R_{o \rightarrow m}$  and  $R_{m \rightarrow o}$  for the original-phase-to-metaphase transition and the metaphase-to-original-phase transition, respectively). When we define  $DT_o$  and  $DT_m$  as the duration times of the original phase and the metaphase,  $\Delta R$ , which is equal to  $R_{o \rightarrow m}$  minus  $R_{m \rightarrow o}$ , can be expressed as shown in equations (6) and (7), which are derived from equation (3).

$$\Delta R = \int_0^{DT_o} \frac{d}{dt} R \, dt = \int_0^{DT_o} (\alpha_o - (\alpha_o + \beta_o)R) \, dt \quad (6)$$

$$-\Delta R = \int_0^{DT_m} \frac{d}{dt} R \, dt = \int_0^{DT_m} (\alpha_m - (\alpha_m + \beta_m)R) \, dt \quad (7)$$

where the subscripts o and m indicate the original phase and the metaphase. The periodic time is the sum of  $DT_o$  and  $DT_m$  if the phase transitions occur quickly enough, and thus the frequency ( $F$ ) can be expressed as equation (8).

$$F = \left( \frac{1}{DT_o + DT_m} \right) \quad (8)$$

By solving these equations, we can predict the shape of the polar plot of the frequency against the angle of the polarisation light. Examples of simulated polar plots are shown in Fig. 2d, Fig. 3c, and Fig. S2a in the SI; an example of the behaviour of  $R$  is shown in Fig. S1 in the SI. The difference between the azimuth of the transition moments of the *trans*-isomer in the original phase and the *cis*-isomer in the metaphase is the main cause of the wide forbidden angle, and the balance between the kinetic coefficients and the azimuths of the transition moments of the *trans*-isomer in the metaphase and *cis*-isomer in the original phase de-symmetrises the curve. For the sake of simplicity, the discussion in the main text is based on the transition moments of the *trans*-isomer in the original phase and the *cis*-isomer in the metaphase.

## Experimental Methods

### Preparation of the co-crystals

Co-crystals of **1** and oleic acid were prepared according to a literature precedence.<sup>[1]</sup> In brief, a mixed dispersion of 1 mg of the *trans*-isomer of 6-[4-(phenylazo)phenoxy]hexanoic acid (**1**) and 1.3 mg of sodium oleate in 1 mL of phosphate-buffered solution (pH = 7.5; 75 mM) was ultrasonicated and incubated at 25 °C for several days to obtain a dispersion of the co-crystals. The dispersion was placed on a glass slide and sealed for observation.

[1] Y. Kageyama, T. Ikegami, S. Satonaga, K. Obara, H. Sato, S. Takeda, *Chem.-Eur. J.* **2020**, *26*, 10759-10768.

### Observation method

For the microscopic observation, a differential interference contrast microscope (TE2000 system, Nikon, Japan) equipped with an epifluorescent unit, which consists of a pre-centred fibre illuminator with a mercury lamp, a BV-1A filter unit ( $\lambda_{\text{ex}} = 435 \pm 10$  nm) and a polariser, and with a Nikon Plan Fluor ELWD 20 $\times$  (NA0.45) objective lens, was used. The excitation photon number was  $6 \times 10^{15}/\text{s}$  for polarised light and  $2 \times 10^{16}/\text{s}$  for non-polarised light, respectively, as measured using a power meter (LP1 Mobiken, Sanwa, Japan). For the experiment shown in Fig. 3, the intensity of the light was reduced by half. A charge-coupled device camera (STC-TC152USB, Sentechna, Japan) was used to record movies at 19.26 fps rate, and Image-Pro Premier software (Media Cybernetics, USA) was used for movie analysis. When more than one oscillation mode was present, the frequency was measured for the long-period oscillation mode. The frame rate of the movies in the SI were processed to be 23.98 fps by using Premier Pro software (Adobe, USA).

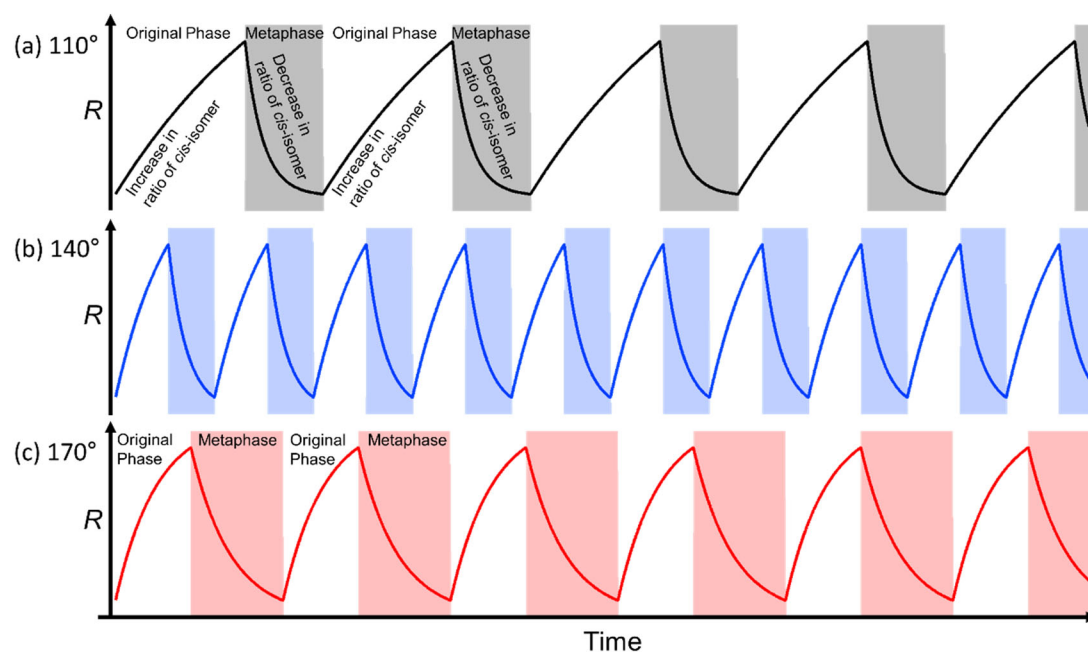


**Fig. S1.** Simulated time profile of the isomer ratio of the generator molecule under irradiation from (a)  $110^\circ$ , (b)  $140^\circ$ , and (c)  $170^\circ$  polarised light, which are consistent with the calculated results shown in Fig. 2d. The coloured regions indicate the metaphase state. The parameters for the simulation were not optimised. The trend in the  $Dr$  (the ratio of the duration time of the metaphase to that of the original phase), as well as the trend in the period, were well simulated.



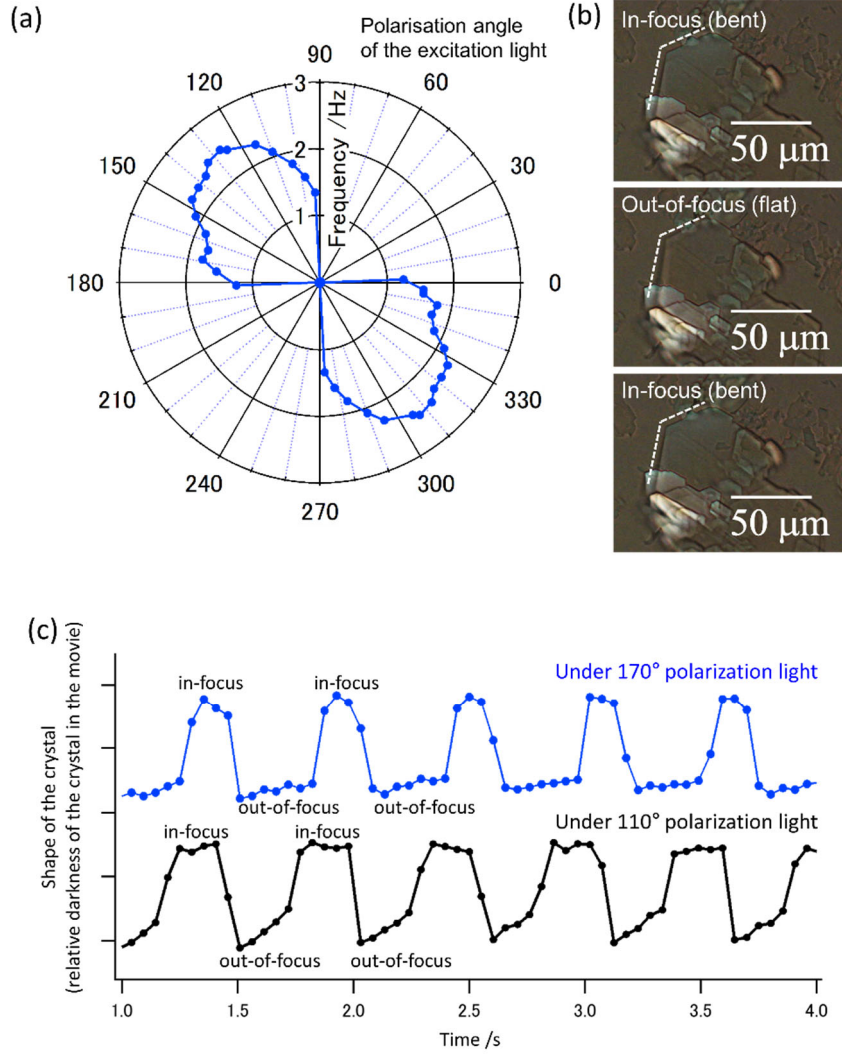


**Fig. S2.** An example of the results of another crystal, corresponding to the results in Fig. 2a–c in the main text. (a) The frequency of the self-oscillation of the crystal under polarised blue light, obtained after irradiation with unpolarised blue light for 5 s. The frequency resolution is approximately 0.05 Hz due to the frame speed of the video used to generate this image (for details, see Movie S7 in the SI). (b) Sequential microscopic images (intervals: 0.21 s) of the oscillatory flipping of the crystal under excitation light with a polarization angle of 145°. The dashed lines are guides for the eye, and the contrast of the pictures was adjusted for clarity. (c) Time profile of the self-oscillation under light with a polarisation angle of 110° and 170°, respectively. The vertical axis is the darkness of the crystal in the movie used to generate this image (for details, see Movie S7 in the SI) and indicates the state of the crystal. For this crystal, the in-focus state is the metaphase and the out-of-focus state is the original phase.

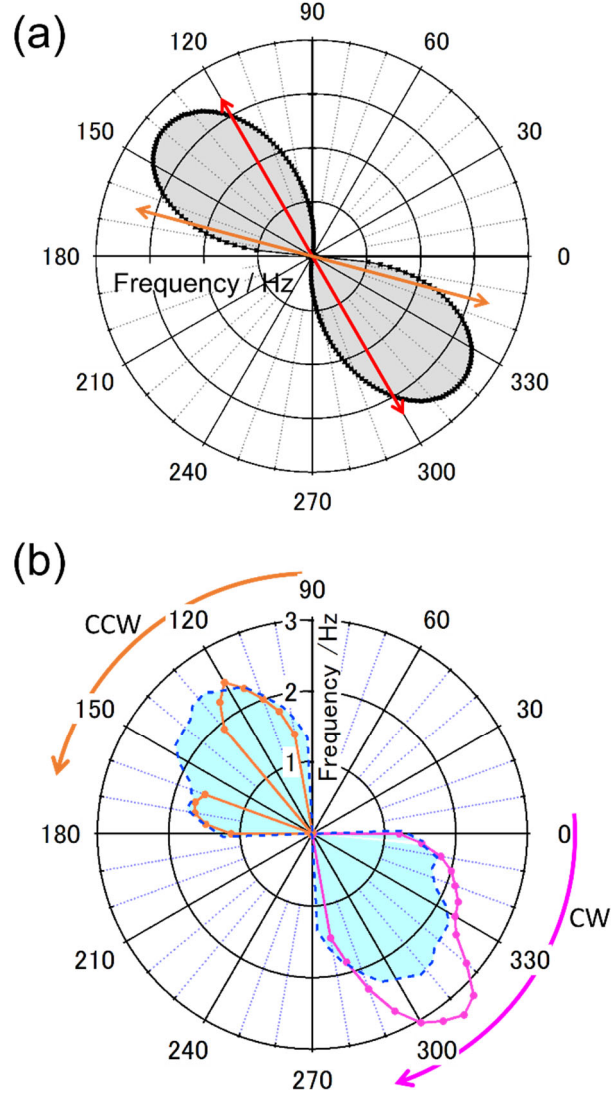


**Fig. S3.** (a) Simulation of the behaviour of the crystal shown in Fig. S2 based on the model shown in the appendix in the main text. Herein, the following values were assigned:  $\theta_{to} = 120^\circ$ ,  $\theta_{co} = 45^\circ$ ,  $\theta_{tm} = 0^\circ$ , and  $\theta_{cm} = 165^\circ$ . The red and orange arrows indicate the direction of  $\theta_{to}$  and  $\theta_{cm}$ , respectively. The other parameters were identical to those for the simulations shown in Fig. 2d and 3c. (b) Frequency of the self-oscillation of the crystal shown in Fig. S2 when the polarization angle of the blue light was changed stepwise, corresponding to the results in Fig. 4 of the main text (for details, see Movie S8 and S9 in the SI). The cyan-coloured area indicates the results shown in Fig. S2.

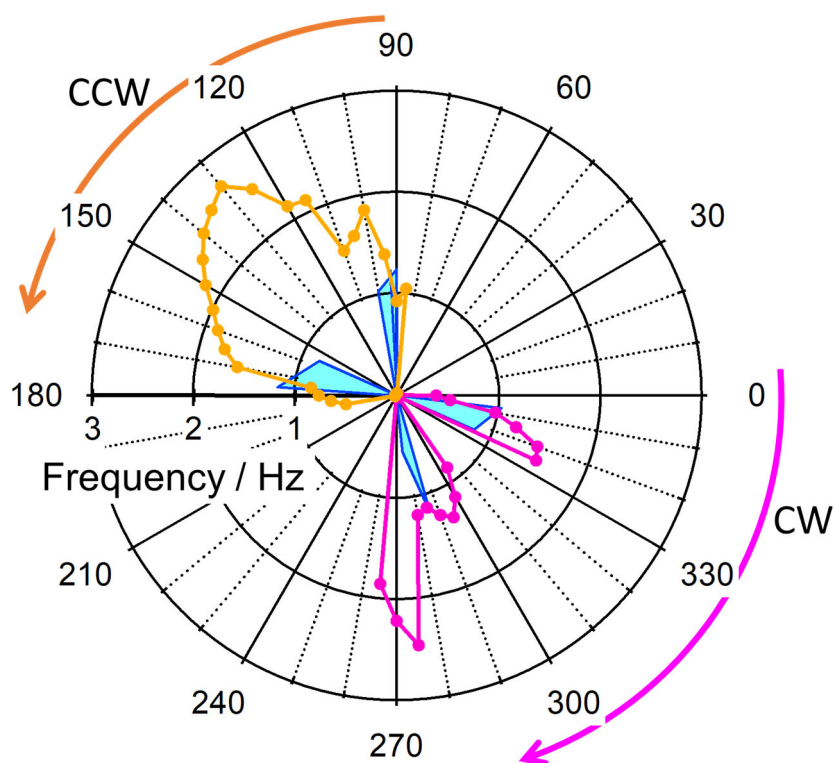


**Fig. S4.** Frequency of the self-oscillation of the crystal shown in Fig. 3 in the main text when the polarization angle of the blue light is changed stepwise (for details, see Movie S5 and S6 in the SI). The cyan-coloured area indicates the results shown in Fig. 3a. The incident light intensity used in the experiment in Fig. 3a was half that used in this stepwise rotation experiment.

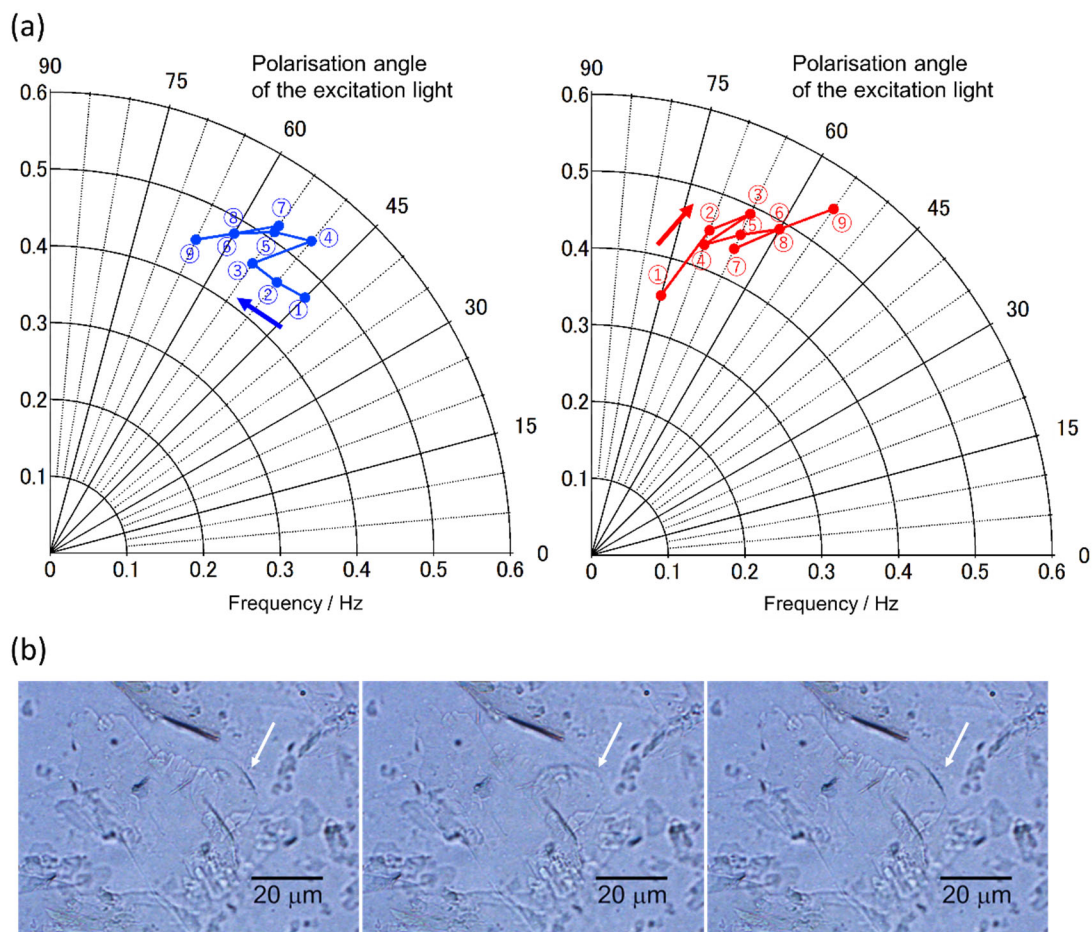


**Fig. S5.** (a) Frequency of the self-oscillation of another crystal when the polarization angle of the blue light is changed back-and-forth (for details, see Movie S10 and S11 in the SI). (b) Micrographs of the crystal, captured without the differential interference contrast unit.